Advanced Composite Materials
Publication details, including instructions for authors and subscription information:
http://www.tandfonline.com/loi/tacm20

High-frequency vibrations on the compaction of dry fibrous reinforcements

Julian Gutiérrez [a], Edu Ruiz [a] & François Trochu [a]
[a] Department of Mechanical Engineering, Chaire sur les Composites à Haute Performance (CCHP), Centre de Recherches en Plasturgie et Composites (CREPEC), Ecole Polytechnique de Montreal, 6079, Montréal, Québec, H3C 3A7, Canada
Published online: 13 Feb 2013.

To cite this article: Julian Gutiérrez, Edu Ruiz & François Trochu (2013) High-frequency vibrations on the compaction of dry fibrous reinforcements, Advanced Composite Materials, 22:1, 13-27, DOI: 10.1080/09243046.2013.764778

To link to this article: http://dx.doi.org/10.1080/09243046.2013.764778

Advanced Composite Materials, 2013
Vol. 22, No. 1, 13–27, http://dx.doi.org/10.1080/09243046.2013.764778

Taylor & Francis
Taylor & Francis Group

High-frequency vibrations on the compaction of dry fibrous reinforcements

Julian Gutiérrez*, Edu Ruiz and François Trochu

Department of Mechanical Engineering, Chaire sur les Composites à Haute Performance (CCHP), Centre de Recherches en Plasturgie et Composites (CREPEC), Ecole Polytechnique de Montreal, 6079, Montréal, Québec, H3C 3A7, Canada

(*Received 26 April 2012; accepted 7 January 2013*)

Liquid Composite Molding (LCM) is a composite manufacturing technique, in which a dry fibrous reinforcement is placed inside a mold, impregnated with a liquid resin and cured. During the fabrication process, the fibrous preform is subject to through-thickness and in-plane deformations. These deformations may affect the quality of the components and their mechanical performance. Hence, the compaction behavior of the reinforcement is crucial in order to predict its deformation during processing. The present work deals with the first stage of LCM manufacturing, during which the dry preform is draped into the rigid base mold and then compressed during closure of the upper mold. Under traditional manufacturing conditions, the preform is subjected to a single static compressive load. In the current study, controlled vibrations are applied to the preform before static compaction. These vibrations have a strong impact on nesting and on the further static compaction behavior of the reinforcement. The scope of this investigation is to study the influence of vibration parameters such as amplitude and frequency on the compaction of continuous fiber beds used to reinforce high-performance composites. Mechanical tests were performed using a special DMA instrument that allows characterizing the dynamic compaction of fibrous reinforcements at high frequency.

Keywords: composites manufacturing; compaction; vibration; nesting

1. Introduction

Liquid Composite Molding (LCM) is a widely used manufacturing technique of composite components of medium and large size. In the past decades, composite materials have had a deep impact in many industrial fields from aeronautics to automotive and sports, leading to the development of a range of new manufacturing techniques. LCM processes consist of injecting a liquid resin through fibrous reinforcements. After resin impregnation, the composite is kept under pressure and then allowed to cure. Three main fields of investigation arise in LCM: the compressibility of the fibrous reinforcement, mold filling, and resin polymerization. The present study focuses on compressibility. Understanding the preform behavior under compressive loads is a key issue to predict the force required to close the mold.[1,2] This permits a proper dimensioning of the clamping press in Resin Transfer Molding (RTM) and allows predicting the fiber volume fraction in Vacuum Assisted Resin Infusion (VARI).[3]

*Corresponding author. Email: julian-andres.gutierrez@polymtl.ca

Besides, the compressibility of fibrous materials has been associated to changes in the fiber bed permeability,[4,5] part thickness,[6] and inter-laminar properties.[7]

During fiber bed compaction at high fiber volume content, the elevated compressive force may create a deformation of the upper mold leading to a nonuniform thickness along the part. This is frequently observed in RTM-light processes, in which the mold is semi-rigid. In high-end applications such as aeronautics, part thickness and fiber volume fraction have to be uniform and well controlled for certification purposes. In such applications, the use of static compaction may not be the best approach for achieving the desired fiber volume content.

In the case of complex parts, it is often required to cut several layers of different shapes that are draped on a double curvature surface. In these applications, overlaps are frequently observed, resulting in a higher number of layers and, hence, a higher fiber volume content (V_f). These local increments of V_f induce stress concentrations during mold closure. For this reason, mold and clamping equipments are over-dimensioned in order to ensure constant thickness of the part and minimize creep deformation. The use of controlled high frequency vibrations can possibly help not only in reducing the variability of V_f, but also to lower the mold deformation and the clamping force.

The idea of using vibrations on composite manufacturing is not new. In fact, the use of compressive pulsations in LCM processes has been the object of recent studies.[8,9] Some investigations found that applying vibrations on the mold during resin impregnation reduces the mold filling time.[10–12] According to these authors, vibrations allow reducing the resin viscosity by shear thinning. Moreover, Muric-Nesic et al. [13] reported that the void content in polymer composites can be reduced when the mold undergoes vibrations after resin saturation. In this case, vibrations are expected to improve air bubble dissolution by buoyancy, contributing to lower void content in parts. Kruckenberg et al. [14] studied the response of dry and lubricated plain weave fabrics (PWF) subjected to repeated compaction. The tests were limited to 10 Hz and conducted with a universal testing machine and have shown that sequential compaction improves the fiber network reorganization, resulting in higher fiber volume fractions. The authors suggest that results can be improved by increasing the number of layers and the compaction frequency, and by using low-viscosity lubricated samples.

The present investigation explores the impact of high frequency vibrations on the compaction response of dry fibrous reinforcements. Contrary to previous studies, in this case, the fabrics are subjected to vibrations before compaction and resin impregnation. Firstly, static compaction tests were carried out on two fiberglass fabrics and the nesting and creep behaviors were analyzed. Secondly, a vibration-assisted technique was implemented to evaluate the impact of vibrations on fabric compaction. Finally, the results of these two different compaction procedures (i.e. static and vibration-assisted) will be discussed and compared.

2. Compaction of fibrous reinforcements

2.1. Geometric and mechanical behavior

Observing the whole compaction process, the interaction among fibers can be studied as long as two or more fabric layers are piled up. At this stage, when no pressure is applied, the layers are in contact with each other in only a very few spots. Friction forces at the contact points between layers prevent yarns from slipping. When a compaction pressure is applied, it overcomes inter-yarn and/or inter-fiber frictional forces and slippage of fibers takes place on two different scales. On the microscopic scale, tow filaments slip into the free space between each other reducing the pores among the fibers and flattening the yarn bundle from their initial configuration into an ellipse of higher aspect ratio.[15] Simultaneously, at the mesoscopic scale, fabric tows slide in the larger available spaces where the stacking structure is not stable. Warp and weft bundles are slightly reoriented to accommodate changes in the local microscopic geometry, giving place to nesting and inter-layer packing. These mechanisms, individually and combined, determine the initial irreversible microstructure of the preform. In these phenomena, thickness reduction comes almost entirely from the apparent compressibility of the interstitial space between yarns, and not from the compressibility of the fiber solid material.[16]

In the pressure–thickness relation of Figure 1, the initial fabric compaction follows a linear regime when the resistance is almost negligible. As compaction pressure continues to increase, a nonlinear behavior takes place. The number of contact points increases with pressure and yarn deformation, while higher inter-fiber friction resists deformation. This is an unstable regime, in which the topology of the fibrous network evolves randomly, changing continuously the number of contact points and the stiffness.[17] Gupta et al. [18] reported that the true contact area in a fibrous material increases exponentially with the load. Once the larger spaces have been filled and the remaining interstitial openings are arranged in a more stable structure, the total deformation results in the compression of the fiber tows.[16] The tows, idealized as sinusoidal waveforms, decrease their amplitude, while the area of their cross section decreases too.[19]

Further increase in pressure leads to the last regime of compaction. At this stage, yarns are mostly flattened, fibers are in contact and the pores of the interstitial spaces become isolated and surrounded by solid material. The compressibility of such enclosed pores is assumed to be a function of the elastic fiber compressibility. In this last stage, the preform geometry at the microscopic level has reached a consistent solid state.[16]

2.2. Fiber nesting

Nesting results from lateral and vertical shifts of fibers inside the yarn and of fiber bundles between neighboring layers (i.e. inter- and intra-layer slippage). Figure 2 shows schematically the geometric effects of nesting on a PWF cross section. In a laminate, nesting is evidenced by a decrement in thickness per layer where the number of layers increases. Consequently, the fiber volume fraction becomes larger when more layers are stacked together.[20]

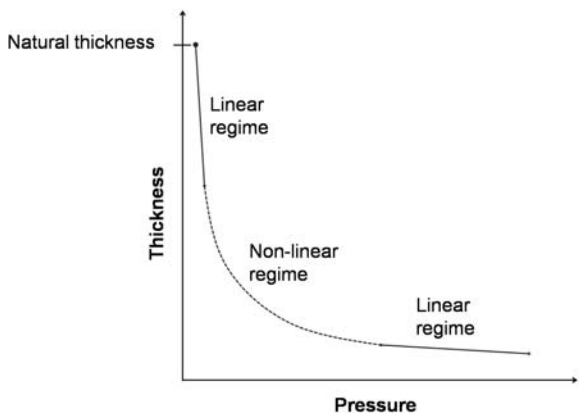

Figure 1. Typical thickness–pressure compaction curve of fibrous material.

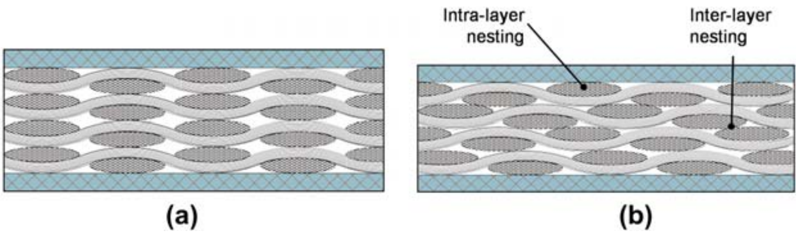

Figure 2. Nesting of plain weave fabric layers: (a) stacked plies; (b) after nesting.

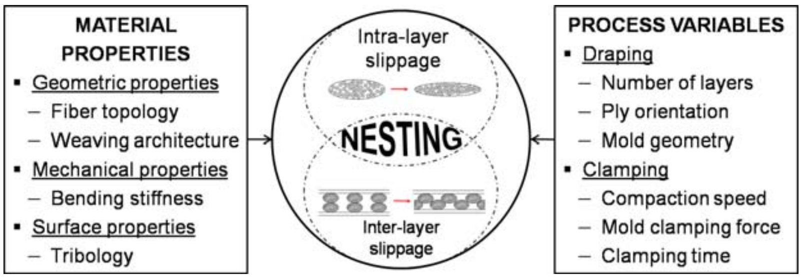

Figure 3. Main factors affecting fiber nesting.

According to numerous authors [21–24] nesting represents one of the most important contributions to preforms compaction.

Nesting has shown to display favorable effects over important factors such as fiber volume fraction, preform springback,[25] inter-laminar shear stress [7] and microcrack propagation.[26] Fabric topology plays a key role on nesting. In fact, it has been demonstrated that certain weaving patterns are more likely to nest than others.[6,20] In addition to the intrinsic fabric 'nestability,' other parameters, such as fiber surface properties and fabric draping, also affect fiber network reorganization. To summarize, fiber properties, preform geometry, and weaving techniques contribute to the tribological conditions that determine whether fiber slippage takes place or not.

Figure 3 sums up the main factors that influence nesting. The intrinsic material properties that cause nesting come from the fiber network topology, the mechanical and/or chemical sizing, and the bending stiffness of fibers. The process variables contributing to nesting are related to draping and mold clamping conditions. Both material properties and process variables contribute to the compaction behavior and to the maximum fiber volume fraction attainable.

3. Materials and experimental techniques

3.1. Testing equipment

In this study, a Dynamical Mechanical Analyzer (*DMA + 450* from *01dB-Metravib*, France) was used to investigate the compaction of two fiberglass fabrics (see Figure 4). This instrument consists of a dynamic shaker capable of imposing sinusoidal strains and stresses to the sample. Frequency and amplitude of the oscillatory input are controlled by the software application *Dynatest*. By measuring the specimen's response in force or deformation, as well as the lag between the stress and strain sine waves, it is possible to calculate the viscoelastic

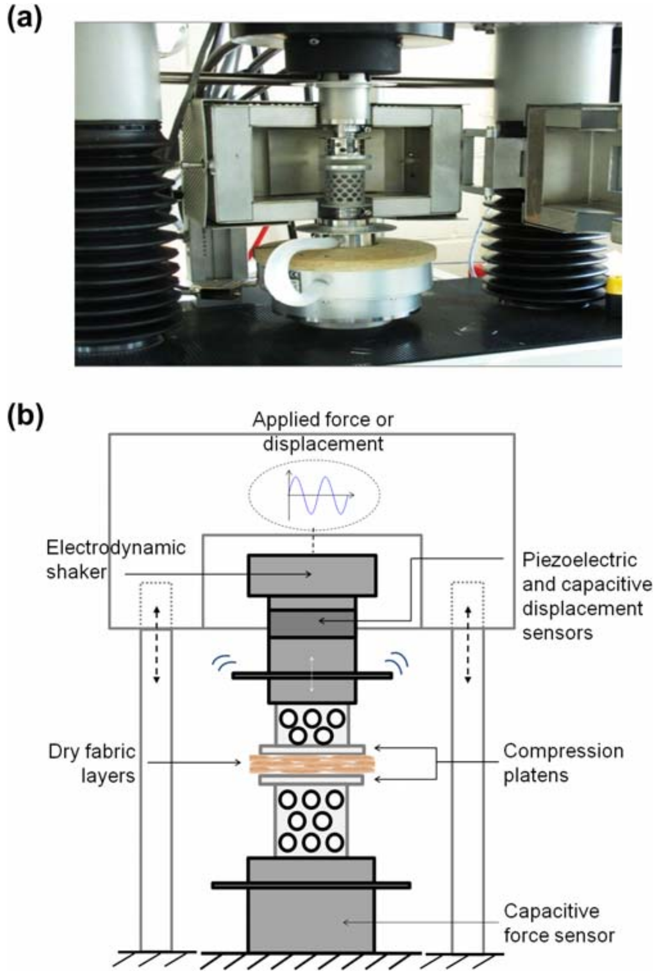

Figure 4. Dynamical Mechanical Analyzer DMA + 450: (a) photograph of the actual instrument and (b) schematic of the apparatus.

properties of the tested material. The *DMA + 450* can reach forces up to 450 N and depending on the specimen's stiffness its frequency ranges from 1×10^{-5} to 1000 Hz.

A static load cell with a capacitive sensor measures the testing force at frequencies up to 400 Hz. For higher frequencies, a piezoelectric force sensor must be employed. Regarding the specimen holder, two circular platens of 40 mm in diameter were used. During testing, the platen attached to the dynamic shaker is limited to a vertical displacement of 6 mm. The strain measurement is carried out alternatively by the capacitive displacement sensor and the piezoelectric sensor.

3.2. Reinforcement materials

In this work, two types of fibrous reinforcements were studied; a Biaxial Non Crimp Fabric (BNCF) and a PWF. Figure 5 presents scanned images of the selected reinforcements. These

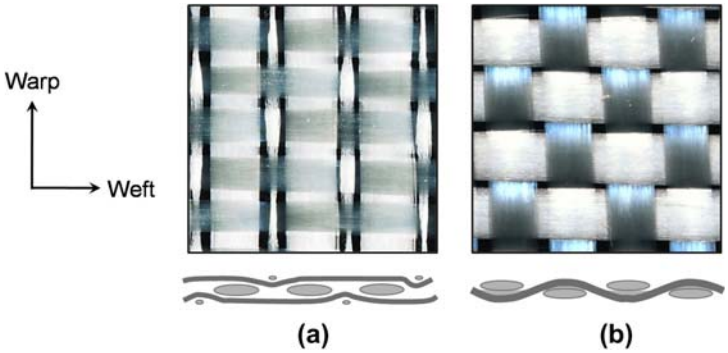

Figure 5. Reinforcing materials investigated: (a) BNCF reinforcement and (b) PWF fabric from JB Martin Ltd.

Table 1. Specifications of reinforcing material.

			Linear density‡ (g/1000 m)		Tow count‡ (ends/cm)	
Material	Areal density (g m^{-2})	Ply thickness† (mm)	Warp	Weft	Warp	Weft
Biaxial noncrimp fabric	500.285 ± 3.06*	0.632 ± 0.006*	735	275	3.1	5.2
Plain weave fabric	588.096 ± 2.21*	0.568 ± 0.014*	750	750	4	3.9

Notes: *Student's (*t*) distribution with a 95% confidence level.†The ply thickness was measured at a compressive pressure of 10 kPa.‡Data from manufacturer.

fabrics supplied by J.B. Martin Ltd. have been woven using the same type of roving material and present similar physical characteristics (see Table 1).

The BNCF reinforcement is made out of three unidirectional E-glass fiber layers arrayed orthogonally (90°/0°/90°) and stitched together using polyester binder filaments in the warp direction. The PWF reinforcement is a balanced fabric, meaning that the same tows are used in the warp and weft directions. However, because of the tensile forces exerted on the warp tows during the weaving process, these are tighter, giving a slightly higher tow count in this direction.

3.3. Compaction experiments

The compaction response of the selected reinforcements has been evaluated through a series of experiments. Firstly, in order to evaluate nesting behavior, static compaction tests were carried out on a single layer as well as on stacks of three and six layers. Secondly, to study the impact of vibrations on compaction, an alternative vibration-assisted compaction technique was carried out with the two fabrics. The tests conducted are described in Figure 6 and Figure 7.

Figure 6 shows the *static compaction and creep tests*. The thickness h_i at rest is measured on the piled layers when no pressure is applied. Then, to assure the contact between the compression platens and the preform before the test, a precompaction pressure of 10 kPa is applied leading to the initial thickness h_0 at time zero. Later, when the compaction pressure reaches 100 kPa, the preform reduces its thickness down to h_1. At last, the pressure is kept

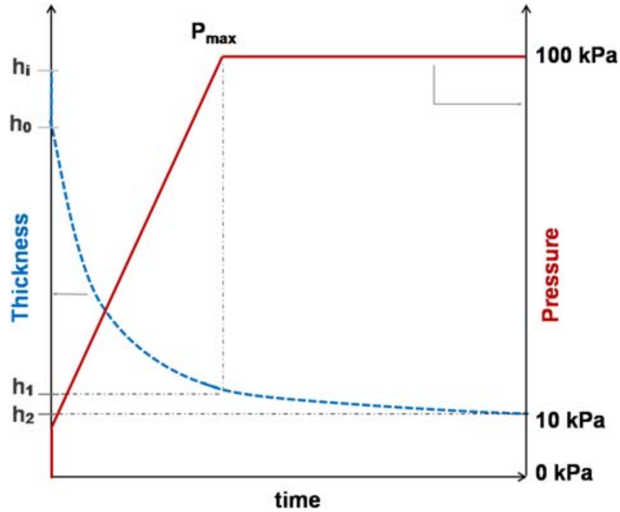

Figure 6. Description of the static compaction followed by creep.

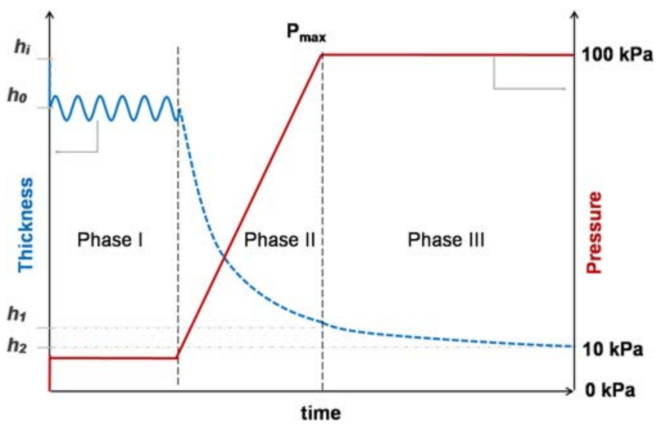

Figure 7. Description of the vibration-assisted compaction and creep.

constant during 2 min to observe the creep behavior of the fibrous material. The final thickness h_2 is obtained at the end of this period.

The *vibration-assisted compaction and creep test* shown in Figure 7 is composed of three phases. In the initial stage (I), the preloaded fibrous material is subjected during 120 s to controlled vibrations at given frequencies and amplitudes. Afterwards in phase II, the 100 kPa static compaction is applied, and at last in phase III, the pressure remains constant during 2 min. Phases II and III reproduce the *static compaction and creep tests* depicted in Figure 6.

Fabric specimens were all cut from the same position in the roll, avoiding the sides where fabrics are often damaged because of handling and storage. A cutting die was used to warranty uniform sample dimensions of 50 mm × 50 mm. After cutting, specimens were carefully placed on the DMA bottom platen, preserving the same warp and weft directions between layers. If during this manipulation any fiber tow is detached from the specimen, the ply was discarded and replaced by a new one. This procedure was followed systematically in order to minimize sample variability. The reported data on each set of experiments represent the arithmetic mean of five successful tests. All tests were performed at room temperature.

The misalignment of DMA platens may induce important variations on the resulting fiber volume fraction. For this reason, the platens' alignment was evaluated using a pressure sensor film to reveal the pressure distribution between the platens when they are in contact. A slight misalignment was observed and then measured using thickness gauges. After some adjustments, this misalignment was reduced from 100 to nearly 35 μm, which is an acceptable tolerance considering that it represents less than 5% of the thickness variation during the compression of a single layer.

4. Results and discussion

4.1. Nesting study

A series of experiments were performed with a single layer as well as with stacks of three and six layers to study the compaction and nesting behavior of the two fabrics investigated. Preforms were compacted at a rate of $5\,\mathrm{mm\,min^{-1}}$, up to a maximum pressure of 200 kPa. The decrease of thickness per layer while increasing the number of layers is a clear evidence of the nesting phenomena. Figures 8 and 9 display these observations for the BNCF and PWF reinforcements, respectively.

Nesting takes place from the beginning of compaction until the maximum pressure is attained. At 200 kPa, the BNCF seems to be able to continue decreasing in thickness at a nonlinear rate (refer to Figure 1). In addition, the gap between the curves for three and six layers is large enough to suppose that further nesting can be attained if the number of layers and pressure increase. The compaction behavior of the PWF is quite different. At 200 kPa, the fabric compaction seems to progress linearly (third regime in Figure 1). Besides, the addition of three to six layers decreases slightly the thickness per layer. This indicates that further nesting would be rather difficult. Figure 10 depicts the increment in fiber volume fraction with the number of layers for both materials. When the number of layers increases from three to six, the BNFC fiber volume fraction grows by 4.2%, while for the PWF, it barely changed (0.5%). Similar observations were reported by Lomov et al. [20] and Saunders et al. [27].

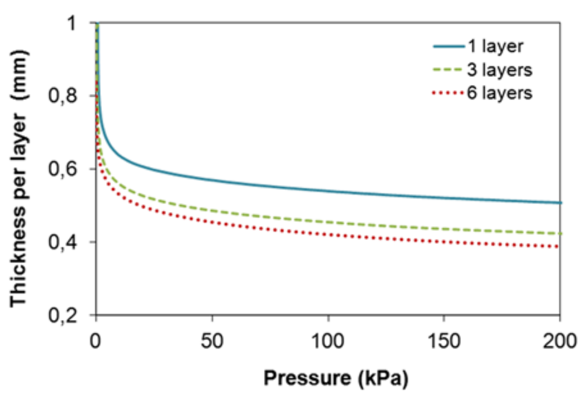

Figure 8. Evolution of the thickness per layer for BNCF preforms containing one, three, and six layers.

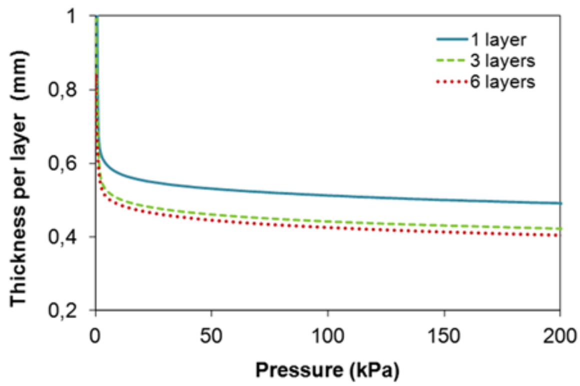

Figure 9. Evolution of the thickness per layer for PWF preforms containing one, three, and six layers.

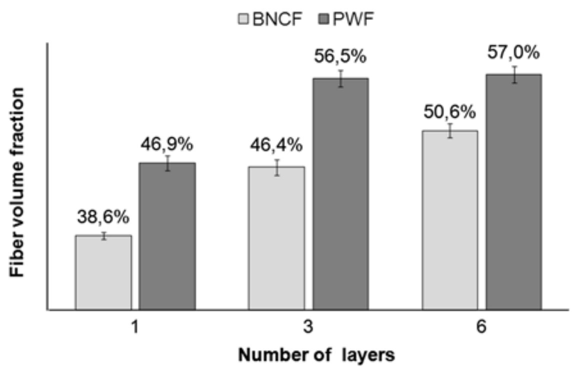

Figure 10. Increase in fiber volume fraction with the number of layers for the PWF and BNCF reinforcements at a compression pressure of 200 kPa.

4.2. Static compaction tests

Static compaction and creep tests reproduce the conditions that dry reinforcements endure during manufacturing processes with a deformable upper mold such as VARI and Light Resin Transfer Molding (LRTM). In these processes, the mold closing force is provided by the atmospheric pressure before resin infusion. Experiments were performed on stacks of four layers of PWF and BNCF using the parameters shown in Table 2.

The fiber volume fraction is calculated at each step by Equation (1) below, where n is the number of layers, A_w the fabric areal density, h_n the thickness of the preform at a given compaction stage, and ρ_f the density of glass fibers.

$$V_f = \frac{n \cdot A_w}{h_n \cdot \rho_f} \tag{1}$$

The two fabrics tested exhibit different compaction behaviors, as shown in Figure 11. The PWF reaches a fiber volume fraction of 54% at 100 kPa while the noncrimp fabric attains only 45% for the same compaction load.

The variation of fiber volume fraction during compaction is divided into three stages as presented in Figure 6. Note that V_{fo} in Figure 11 corresponds to h_0 in Figure 6; the same for

Table 2. Parameters of the compaction and creep tests.

Number of layers	Preload (kPa)	Compaction speed ($N\ s^{-1}$)	Max. pressure (kPa)	Creep time @ 100 kPa (s)
4	10	10	100	120

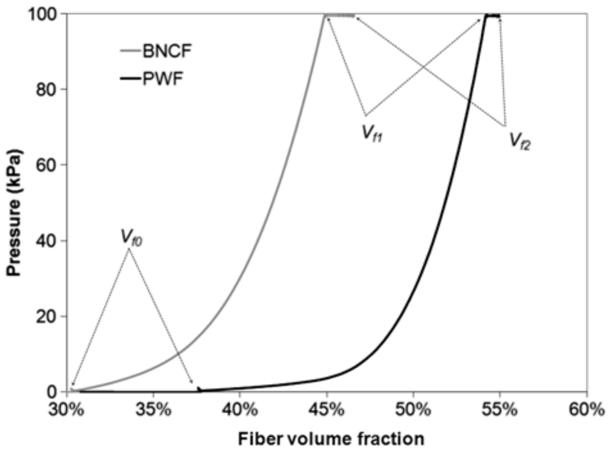

Figure 11. Results of static compaction tests on the two reinforcements investigated.

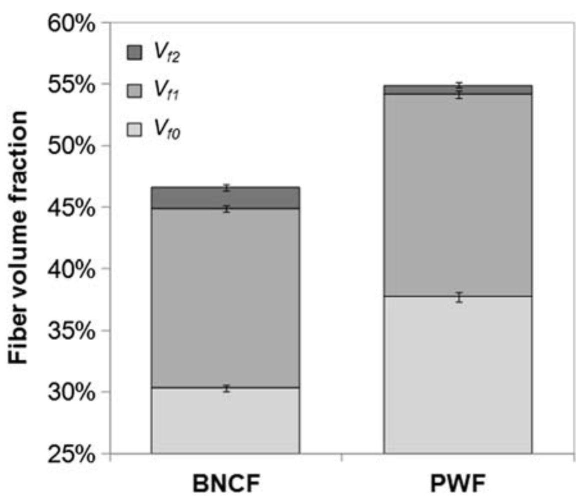

Figure 12. Increment in fiber volume fraction after static compaction.

V_{f1} and V_{f2} which correspond to h_1 and h_2, respectively. Figure 12 depicts the variations of fiber volume content for each reinforcing material during static compaction. Both fabrics have a natural V_f of around 25% when no pressure is applied. After an initial precompaction load of 10 kPa, the initial fiber volume content V_{fo} reaches 30% for the BNCF, and 37% for the PWF. After compaction at 100 kPa, the same behavior is observed for both fabrics. However, a difference occurs during the creep stage indicating that more relaxation takes place with the BNCF than with the PWF. This behavior is probably due to the spring effect of woven fabrics rather than pure nesting between fibers.

4.3. Vibration-Assisted compaction tests

The vibration-assisted compaction test consists of applying a vibration excitation to the fabrics prior to compaction (see Figure 7). Three compaction frequencies were tested and combined with two different amplitudes. As described in Table 3, the tested amplitudes for the first two frequencies (10 and 100 Hz) were 50 and 100 µm, while for the higher frequency (300 Hz), amplitudes of 50 and 80 µm were applied. As a matter of fact, at 300 Hz, the DMA limits the maximum amplitude to 80 µm. In all cases, steady vibrations were imposed during 120 s. During the second phase, static compaction and creep tests were performed exactly as in the set of first experiments. Figures 13 and 15 display the results of these experiments for the BNFC and PWF, respectively.

Figure 13 shows that applying the vibration-assisted technique to the BNCF increases V_f by nearly 2.5%. Most importantly, if a V_f of 45% is desired for a composite part, it will normally require a clamping force of 100 kPa on the mold. By applying the vibratory precompaction, the clamping force can be reduced to 70 kPa. A 30% smaller force means that less stiffness is required for the mold and less energy is spent to close it. Figure 14 shows the

Table 3. Parameters used in the vibration-assisted compaction and creep tests.

Preform		Phase I (120 s)				Phase II		
Fabric	No. of layers	Preload (kPa)	Frequency (Hz)	Amplitude (µm) (a)	Amplitude (µm) (b)	Compaction speed ($N\ s^{-1}$)	Max. pressure (kPa)	Creep time @ 100 KPa (s)
BNFC	4	10	10	50	100	10	100	120
			100	50	100			
PWF			300	50	80			

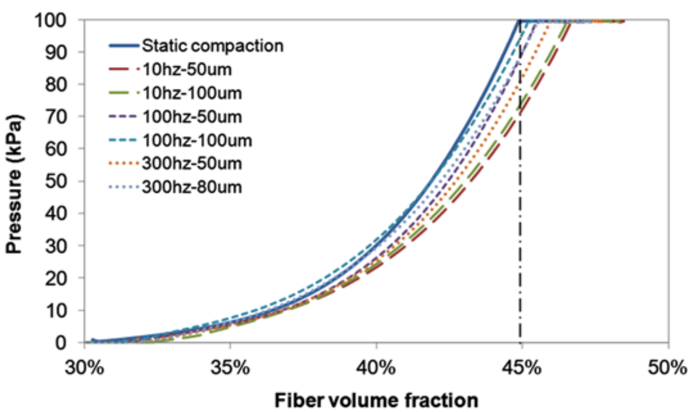

Figure 13. Results of the vibration-assisted compaction for the BNCF.

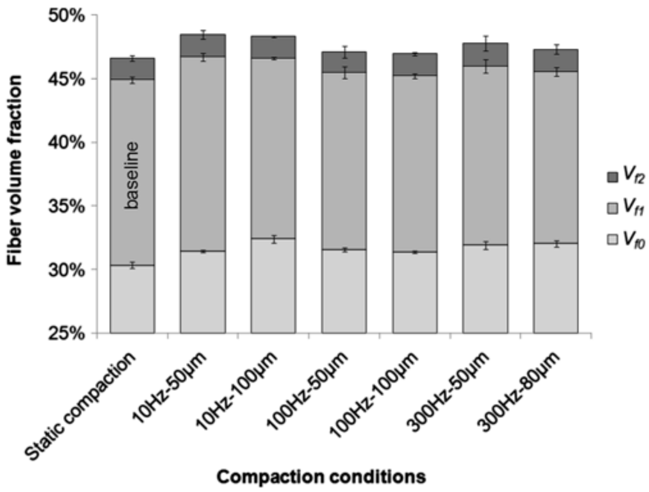

Figure 14. Increment in fiber volume fraction during static and vibration-assisted compaction for the BNCF reinforcement.

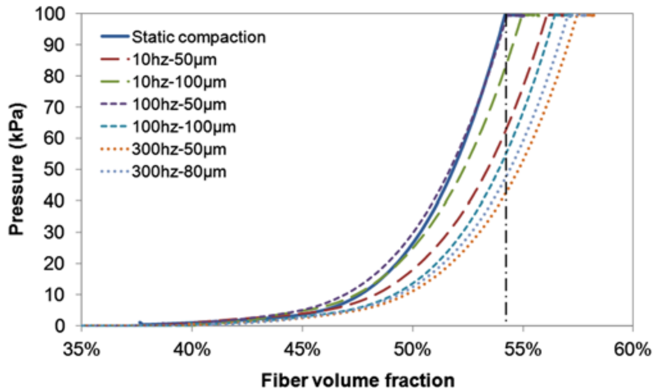

Figure 15. Results of vibration-assisted compaction tests for the PWF reinforcement.

fiber volume fraction attained after different vibration conditions. During the precompaction stage at 10 kPa it was observed that applying a vibration-assisted excitation increases the fiber volume fraction V_{fo} compared to the baseline (static compaction). This can be explained by the vibrations that promote inter- and intra-layer slippage, and hence induce premature nesting. The higher increment was found for frequencies of 10 and 300 Hz. These results show that the amplitude of oscillation has no real influence on V_f. Only a slight variation can be observed for tests at 10 Hz for amplitudes of 50 and 100 µm. The final fiber volume fraction after the compaction stage II (V_{f1}) shows a similar behavior. The last compaction stage (V_{f2}) during the creep period indicates that the gain in fiber volume content is the same whether static or vibration-assisted compaction is carried out. This means that vibrations affect the way and speed of fiber reorganization, but have no impact on creep.

The PWF displays a similar behavior as the BNCF when subjected to vibration-assisted compaction (see Figure 15). In this case, the impact of vibrations on the compaction curve is higher than for the previous reinforcements with a reported increase of 3.2% on V_f. Moreover,

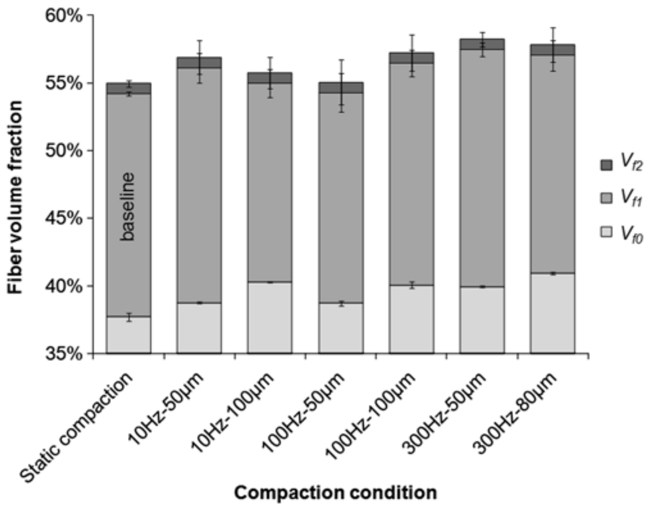

Figure 16. Increment in fiber volume fraction during static and vibration-assisted compaction for the PWF reinforcement.

the force usually required to reach a V_f of 54% under static compaction is reduced from 100 to 40 kPa with the vibration-assisted technique.

Figure 16 presents a detailed analysis of the compaction process for the PWF fabric. The precompaction stage at 10 kPa shows an initial fiber volume fraction V_{fo} that varies with vibration frequency and amplitude. Contrary to the BNCF reinforcement, where the amplitude of oscillation has no impact on V_f, for the PWF, the higher amplitude has an effect on V_{fo}. Nevertheless, this influence is not observed during the final stages of compaction. In fact, there is no clear influence of amplitude on V_{f1}. Moreover, the high variability observed on V_{f1} makes difficult to reach any conclusion on this matter. Regarding the frequency, it is observed that vibrations at 300 Hz gave the highest fiber volume fraction V_{f1}. Finally, creep does not seem to be affected by vibration-assisted compaction. We infer that vibrations are at the origin of fibers rearrangement. In the PWF fabric, this reorganization seems to be unstable probably due to nesting and also vibrations. This results in a higher thickness variability.

The impact of frequency and amplitude might be altered by a temporary loss of contact between the upper platen and the specimen. If the first vibrations have deformed permanently the fibrous material, then the preload of 10 kPa was probably too small to follow this deformation. For this reason, the two elements might have lost contact. In order to prevent an eventual separation between the compression platens and the fibrous sample and apply vibrations more efficiently, it is recommended in future investigations to use force and frequency-controlled vibrations.

5. Conclusions

This investigation aimed to study the compaction behavior of fibrous reinforcements subjected to vibration loads. Two common glass fabrics of J.B. Martin were used: the PWF and BNCF reinforcements. Initially, a constant speed compaction test was used to evaluate the intrinsic characteristics of several stacks of the two reinforcements investigated. It was found that a larger number of layers increased nesting, which translates into a larger fiber volume fraction V_f or a reduced thickness per layer. The BNCF reinforcement seems to increase nesting proportionally from one to six layers. The PWF seems to stabilize nesting after six layers (i.e. more layers will not increase nesting). The compaction was followed by a dwell at constant pressure in order to study the creep behavior. More creep is observed for the BNCF than the PWF, probably because of the spring effect of woven fiber tows in the PWF fabrics.

Secondly, a high-frequency DMA instrument was used to apply a controlled frequency excitation to the samples prior to compaction. Vibration-assisted compaction tests were performed at different frequencies and amplitudes. The application of such high frequency vibrations to fiber beds improved their compressibility.

The experiments carried out for different vibration frequencies show a clear impact on fiber nesting, but amplitude seems to have a minor effect. The experimental results presented in this paper revealed the positive influence of vibrations on fabric compressibility. However, because of the stochastic nature of fiber nesting, it was difficult to evaluate the gain quantitatively. For instance, while for the BNCF reinforcement the compaction response seems to be independent of the vibration amplitude, no predictable behavior could be observed for the PWF fabric. In fact, although vibrations had a stronger influence on the PWF than on the BNCF, a higher variability probably connected to nesting was observed for the PWF.

Acknowledgments

The authors gratefully acknowledge financial support from the Chair of Composites of High Performance (CCHP) Canada Research Chair and the Natural Science and Engineering Research Center (CNSERC) of Canada. The authors also thank R. Barbin from 01-dB Metravib for his support with the DMA and J.B. Martin Ltd. for providing the fabrics used in this investigation.

References

[1] Robitaille F, Gauvin R. Compaction of textile reinforcements for composites manufacturing. I: review of experimental results. Polym. Compos. 1998;19:198–216.

[2] Gauvin R, Chibani M. Modelization of the clamping force and mold filling in resin transfer molding. In: Proceedings – Technical Sessions of the 43rd Annual Conference, Composites Institute; 1988 Feb 1–5; Cincinnati (OH): Publ by SPI.

[3] Trochu F, Ruiz E, Achim V, Soukane S. Advanced numerical simulation of liquid composite molding for process analysis and optimization. Compos. A Appl. Sci. Manuf. 2006;37:890–902.

[4] Croteau-Labouly B. Caractérisation combinée de la pérmeabilité et de la compaction des renforts fibreux dans les procédés de fabrication des composites par infusion. Génie Mécanique. École Polytechnique de l'Université de Montréal. 2007; p. 157.

[5] Demaria C, Ruiz E, Trochu F. In-plane anisotropic permeability characterization of deformed woven fabrics by unidirectional injection. Part I: experimental results. Polym. Compos. 2007;28 (Compendex):797–811.

[6] Saunders RA, Lekakou C, Bader MG. Compression in the processing of polymer composites 1. A mechanical and microstructural study for different glass fabrics and resins. Compos. Sci. Technol. 1999;59:983–993.

[7] Shady E, Gowayed Y. Interlaminar shear stress distribution between nested layers of plain weave composites. Polym. Compos. 2010;31:1838–1845.

[8] Ruiz E, Briones L, Allard E, Trochu F. Flexible Injection: a novel LCM technology for low cost manufacturing of high performance composites. Part I: experimental investigation. In: 9th Int. Conf. on Flow Proc. in Comp. Mat. (FPCM-9); 2008: Montréal (Québec), Canada.

[9] Abdellaoui C. Étude expérimentale du contrôle en pression et en température de la fabrication de composites par injection flexible, in Mechanical Engineering. Ecole Polytechnique de Montréal. 2009; p. 182.

[10] Pantelelis N. Evaluation of the vibration assisted RTM technique in the production of real parts. In: 7th Int. Conf. for Flow Proc. in Comp. Mat; 2004; Delaware, USA.

[11] Gibson R, Ayorinde EO, Yang S, Baig B. Measurement of mold filling times in vibration-assisted liquid composite molding. In: 11th Annual Technical Conference of the American Society for Composites; 1996. p. 768–776.

[12] Song F. Numerical simulation of vibration-assisted liquid composite molding, in mechanical engineering. Detroit (MI): Wayne State University; 2004. p. 183.
[13] Muric-Nesic J, Compston P, Stachurski ZH. On the void reduction mechanisms in vibration assisted consolidation of fibre reinforced polymer composites. Compos. A Appl. Sci. Manuf. 2011;42:320–327.
[14] Kruckenberg T, Ye L, Paton R. Static and vibration compaction and microstructure analysis on plain-woven textile fabrics. Compos. A Appl. Sci. Manuf. 2008;39:488–502.
[15] Steenkamer D. The influence of preform design and manufacturing issues on the processing and performance of resin transfer molded composites. Vols. I and II, Mechanical engineering. Newark (DA): University of Delaware; 1994. p. 477.
[16] Chen B, Cheng AHD, Chou TW. Nonlinear compaction model for fibrous preforms. Comp. – Part A: Appl. Sci. Manufact. 2001;32:701–707.
[17] Toll S, Manson JAE. Elastic compression of a fiber network. J. Appl. Mech. Trans. ASME. 1995;62:223–226.
[18] Gupta BS, El Mogahzy YE. Friction in fibrous materials. Part I. Structural model. Textile Res J. 1991;61(Compendex):547–555.
[19] Chen B, Lang EJ, Chou TW. Experimental and theoretical studies of fabric compaction behavior in resin transfer molding. Mater. Sci. Eng., A 2001;317:188–196.
[20] Lomov SV, Verpoest I, Peeters T, Roose D, Zako M. Nesting in textile laminates: geometrical modelling of the laminate. Compos. Sci. Technol. 2003;63:993–1007.
[21] Chen B, Chou T-W. Compaction of woven-fabric preforms: nesting and multi-layer deformation. Compos. Sci. Technol. 2000;60:2223–2231.
[22] Chen Z-R, Ye L. A micromechanical compaction model for woven fabric preforms. Part II: multilayer. Compos. Sci. Technol. 2006;66:3263–3272.
[23] Somashekar AA, Bickerton S, Bhattacharyya D. An experimental investigation of non-elastic deformation of fibrous reinforcements in composites manufacturing. Compos. A Appl. Sci. Manuf. 2006;37:858–867.
[24] Robitaille F, Gauvin R. Compaction of textile reinforcements for composites manufacturing. III: reorganization of the fiber network. Polym. Compos. 1999;20:48–61.
[25] Somashekar AA, Bickerton S, Bhattacharyya D. Exploring the non-elastic compression deformation of dry glass fibre reinforcements. Compos. Sci. Technol. 2007;67:183–200.
[26] Jortner J. Microstructure of cloth-reinforced carbon-carbon laminates. Carbon 1992;30:153–163.
[27] Saunders RA, Lekakou C, Bader MG. Compression and microstructure of fibre plain woven cloths in the processing of polymer composites. Compos. A Appl. Sci. Manuf. 1998;29:443–454.